# POSTSTACK TIME MIGRATION VELOCITY ANALYSIS BY CRS DIFFRACTION STACKING

*S. Dell and D. Gajewski*

**email:** *sergius.dell@zmaw.de*
**keywords:** *Time migration velocity analysis, imaging, CRS diffraction stack*

## ABSTRACT

*The Common Reflection Surface stack provides the stacked section as well as kinematic wavefield attributes. The importance of this attributes is more and more recognized by identifying more and more application for them. We demonstrate a new application of the kinematic wavefield attributes for the time migration analysis. On the synthetic data we show, how this attributes can be used to effectively separate reflected and diffracted energy. After separating the diffracted wavefield we introduce a technique for poststack time migration velocity analysis. We image the diffraction only data with optimally chosen velocities based on a focussing criterium. The objectives of this work are velocity analysis implemented in the poststack domain and producing highly focused time migrated images. Due to the application in the poststack data domain the presented procedure is stable and fast.*

## INTRODUCTION

Reflected seismic waves as well as diffracted seismic waves are usually recorded during the data acquisition. The conventional seismic processing is tuned to enhancing and imaging reflected waves while the diffracted waves are considered as noise. However, the diffracted waves indicate the presence of small subsurface features or discontinuous structural changes. The identification of this features can be essential, e.g. for the geological interpretation in carbonate environments (Landa and Shemere, 1997; Moser and Howard, 2008) and in salt environments.

The importance of using diffractions in seismic imaging has long been recognized. Harlan et al. (1984) used forward modeling and local slant stacks for extracting velocity information from diffractions. Landa et al. (1987) proposed to construct a common-diffraction-point section by stacking the signal along a diffraction hyperbola and detecting local heterogeneity. Khaidukov et al. (2004) used reflection-stack type of migration to mute the reflection waves from the full wavefield and defocus the residual wavefield in a shot gather. The focusing-muting-defocusing method allows to image small-size scattering objects. Fomel et al. (2006) proposed separation of diffractions appearing on stacked sections for effective migration velocity analysis. Their separation is based on application of plane-wave destruction filters (Fomel, 2002).

We introduce an approach for extracting of diffraction events using the Common Reflection Surface (CRS) stack (Tygel et al., 1997). The CRS stack is a multi-parameter stacking technique. For 2-D media the traveltime $t$ of reflection events is described by three parameters: the angle of emergence $\alpha$ of the zero offset (ZO) ray, the radius of curvature of the normal (N) wave $R_N$ and the radius of curvature of the normal-incidence-point (NIP) wave $R_{NIP}$. In the following this parameter triplets are referred to as the kinematic wavefield attributes. We show that the kinematic wavefield attributes allow to separate reflection and diffraction events in the stacked data. Then we perform poststack migration velocity analysis on the diffraction only data. We make use of diffraction-event focusing as a criterion for migration velocity analysis. The determined velocity model can be used for the update of the time migration velocity as well as for the time migration of the diffraction only data. Finally we image diffraction only data using the determined

velocity model. We use synthetic examples to verify the proposed method. From a practical point of view, the presented procedure is stable and fast producing highly focused time migrated result.

## METHOD

### CRS diffraction stack

The CRS stacking operator is commonly used for the approximation of the reflection response. The kinematic reflection response is given as

$$t^2(m,h) = \left[ t_0 + \frac{2m \sin \alpha}{v_0} \right]^2 + \frac{2t_0 \cos^2 \alpha}{v_0} \left[ \frac{m^2}{R_N} + \frac{h^2}{R_{NIP}} \right], \tag{1}$$

where $h$ is half source-receiver offset, $m$ is the midpoint displacement with respect to the considered CMP position, $t_0$ corresponds to the ZO two-way traveltime (TWT), $\alpha$ is the angle of emergence of the ZO ray, $R_N$ is the radius of curvature of the normal wave, $R_{NIP}$ is the radius of curvature of the NIP wave and $v_0$ is the near surface velocity. However, the kinematic reflection response can be used to estimate the diffraction response as well. According to the CRS stack approach the diffraction point is associated to the reflector with an infinite curvature and an undefined orientation. This implies, for scattering points the radius $R_N$ coincides with the radius $R_{NIP}$ (Mann, 2002). The normal ray down to such reflector is a possible raypath for the diffraction wavefront and the emergence angle along the normal ray is the same as for a scattering point. The kinematic wavefield attribute can be also used to compute the CRS diffraction operator, that approximates the diffractions up to the second order. The estimation of the kinematic response for the scattering point is then given as

$$t^2 = \left[ t_0 + \frac{2m \sin \alpha}{v_0} \right]^2 + \frac{2t_0 \cos^2 \alpha}{v_0 R_{NIP}} \left[ m^2 + h^2 \right], \tag{2}$$

i.e. it depends only on two attributes.

### The diffraction filter

The equality of the both radii $R_{NIP}$ and $R_N$ for diffractions can be used to determine and separate seismic events. We introduce the following function

$$W_F = e^{-\frac{|R_N - R_{NIP}|}{|R_N + R_{NIP}|}} \tag{3}$$

If the radii $R_N$ and $R_{NIP}$ are close to each other, i.e. for diffractions, the function $W_F$ will be close to one or one. If the radius $R_N$ is higher than the radius $R_{NIP}$ as for reflections, the function $W_F$ will be close to zero. Now one can construct the following filter: if the function $W_F$ is equal one, one weights the amplitude with one. In the opposite case one weights the amplitude with zero. However, in most cases we can not exactly determine the kinematic wavefield attributes from data, we rather estimate them. To stabilize the filter operator one uses a threshold of the function $W_F$. We weight the amplitude with one, if the function $W_F$ is above the threshold. The designed filter can then be applied for the stacked data. The events supposed to be reflection events will be suppressed, the events supposed to be diffraction events will not be changed. The stack will contain predominantly diffraction energy.

### Poststack velocity analysis

In the next step we perform migration velocity analysis on the diffraction stacked data. For each point in the image we stack the data along the diffraction trajectory using different migration velocities and determine how well the diffraction events are focused. The diffraction trajectory is given by the double square root (DSR) equation (Hagedoorn, 1954).

$$t_D = \sqrt{\frac{t_0^2}{4} + \frac{(m-h)^2}{v^2}} + \sqrt{\frac{t_0^2}{4} + \frac{(m+h)^2}{v^2}} \tag{4}$$

where $h$ is half source-receiver offset, $m$ is the midpoint displacement with respect to the considered CMP position, $t_0$ corresponds to the zero offset two-way traveltime and $v$ is the migration velocity. For the poststack section the DSR equation simplifies to

$$t_D = \sqrt{t_0^2 + \frac{4m^2}{v^2}} \qquad\qquad (5)$$

As the measure of focusing we use the semblance norm introduced by Taner and Koehler (1969).

$$S = \frac{1}{M} \frac{\sum_t \left( \sum_{i=1}^M f_{i,t(i)} \right)^2}{\sum_t \sum_{i=1}^M f_{i,t(i)}^2}, \qquad\qquad (6)$$

where $f_{i,t(i)}$ are seismic signal amplitudes inside a window of size $M$. The velocity with the highest semblance value will be assumed as to be the searched migration velocity.

## RESULT

In order to demonstrate the potential of the diffraction separation and poststack velocity analysis, it is applied to the synthetic data.

### Synthetic model with 4 scattering points

Figure 1a displays a stacked section of a synthetic model containing five layers and four scattering points. The velocity within the layer is constant. The velocity in the first layer is 1500 m/s, in the second layer 1580 m/s, in the third layer 1690 m/s, in the fourth layer 1825 m/s and in the fifth layer 2000m/s. Four small lenses in the fourth layer produce diffraction events. Applying the designed filter to the stacked section we obtained the corresponding sections containing predominantly diffraction energy (Fig. 1b). We used 0.9 as the threshold for the filter. This threshold corresponds to $R_{NIP} \approx 0.8 R_N$. The diffractions are well separated from reflections event in the areas of conflicting dips. The diffraction only section is now used for the estimation of their migration velocities. For each sample in the ZO section we applied the coherence analysis. Figure 2 illustrates the velocity spectra. The illustrated CMPs are located directly over the scattering points. Figure 2 shows the coherence values as a function of velocity. The time was manually picked and corresponds the maximum of the coherence value. One observes sharp and narrow maxima for the apexes of the diffractions. Figure 3 shows the time migrated sections obtained by Kirchhoff poststack migration with the RMS velocity (a) and with the velocity estimated on the poststack data (b). The RMS velocity was obtained with conventionally velocity analysis for the full wavefield data. The diffractions are focused at the lenses in both cases. However, in the section obtained with the velocity estimated on the poststack data the diffraction energy is better focused.

### Sigsbee2a

Figure 4a shows the stacked section of the full wavefield for the synthetic Sigsbee2a model. Sigsbee 2A is a synthetic constant density acoustic data set released in 2001 by the "SMAART JV" consortium. Sigsbee2A models the geologic setting of the Sigsbee escarpment in the deep water Gulf of Mexico. Irregular boundaries of the salt body cause strong diffractions in the right part of the section. In the left part of the section diffractions are caused by point scatters. Figure 4b illustrates the stacked section after the application of the designed filter. A threshold of 0.85 was used for the filter. This threshold corresponds to $R_{NIP} \approx 0.7 R_N$. On the diffraction only stack we applied migration velocity analysis. With the estimated velocity we performed poststack Kirchhoff time migration. Figure 6 shows the time migrated image of the diffraction only data. The diffractions in the right part of the section are focused to point scatterers (Fig. 6a). Sharp edges of the salt body can be clearly observed in the section as well (Fig. 6b).

## CONCLUSIONS

Using CRS wavefield attributes we have developed a method to separate seismic diffractions from reflections. We constructed a filter based on the fact that the radius of the normal wave $R_N$ should be equal to the
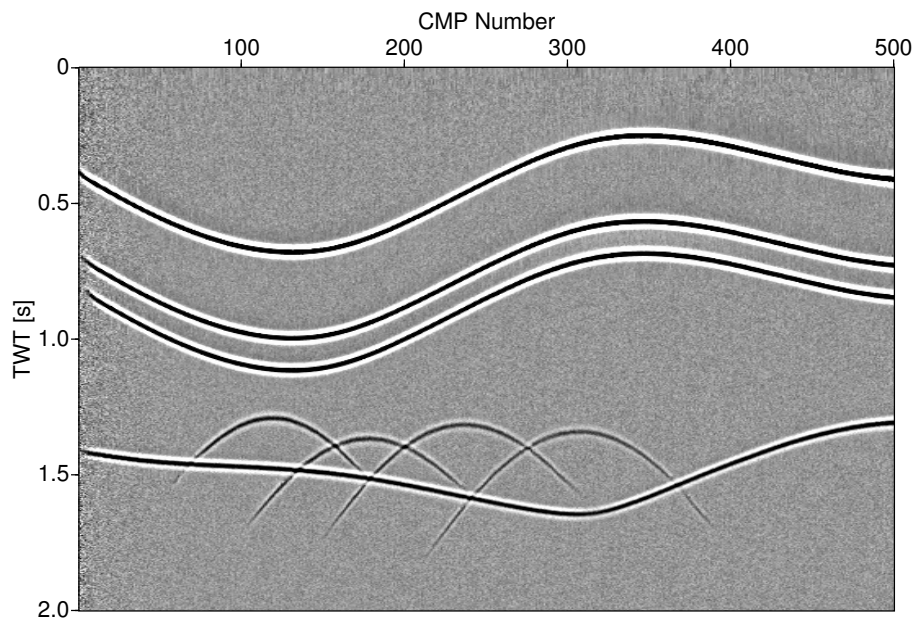
(a)
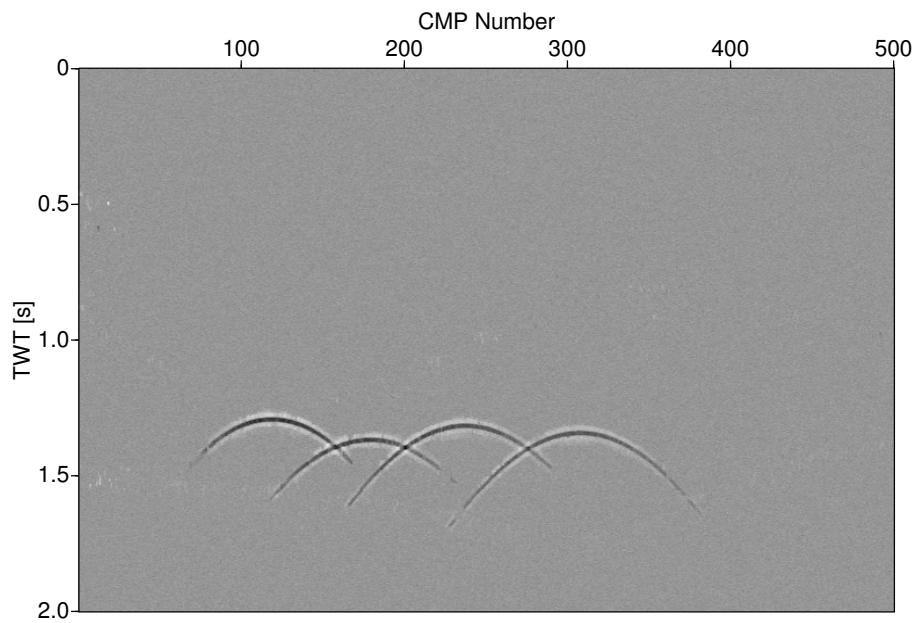


(b)

**Figure 1:** Stacked section of the full wavefield (a) and diffraction only data (b) for the synthetic model with 4 scatter points. Note the different scaling

radius of the normal-incidence-point wave $R_{NIP}$ for diffractions. We then used the separated diffracted wavefield for migration velocity analysis using a focusing criterion. As the measure of focusing we used the semblance norm. Finally we imaged diffraction only data using the determined velocity model. The presented technique represents a fast and stable method for poststack time migration velocity analysis.

The developed method has assumed 2-D data. These concepts may also be generalized to three dimensions by designing 3-D diffraction filter. Also the time-to-depth conversion may be applied for the diffraction only data. The conversion algorithm can be divided in two steps: NIP image wave tomography and post-stack depth migration.

## ACKNOWLEDGMENTS

## REFERENCES

Fomel, S. (2002). Applications of plane-wave destruction filters. *Geophysics*, 67:1946–1960.

Fomel, S., Landa, E., and Taner, M. T. (2006). Posstack velocity analysis by separation and imaging of seismic diffractions. *Geophysics*, 72:U89–U84.

Hagedoorn, J. (1954). A process of seismic reflection interpretation. *Geophys. Prosp.*, 2:85–127.

Harlan, W. S., Claerbout, J. F., and Rocca, F. (1984). Signal/noise separation and velocity estimation. *Geophysics*, 49:1869–1880.

Khaidukov, V., Landa, E., and Moser, T. J. (2004). Diffraction imaging by focusing-defocusing: An outlook on seismic superresolution. *Geophysics*, 69:1478–1490.

Landa, E. and Shemere, K. (1997). Seismic monitoring of diffraction images for detection of local hetero-geneities. *Geophysics*, 63:1093–1100.

Landa, E., Shtivelman, V., and Gelchinsky, V. (1987). A method for detection of diffracted waves on common-offset sections. *Geophysical Prospecting*, 35:359–373.

Mann, J. (2002). *Extensions and applications of the Common-Reflection-Surface Stack method*. Logos Verlag, Berlin.

Moser, T. J. and Howard, C. B. (2008). Diffraction imaging in depth. *Geophysical Prospecting*, 56:627–641.

Taner, M. and Koehler, F. (1969). Velocity-spectra digital computer derivation and applications of velocity functions. *Geophysics*, 34:859–881.

Tygel, M., Mueller, T., Hubral, P., and Schleicher, J. (1997). Eigenwave based multiparameter traveltime expansions. In *Expanded Abstracts*, pages 1770–1773. 67th Annual Internat. Mtg., Soc. Expl. Geophys.
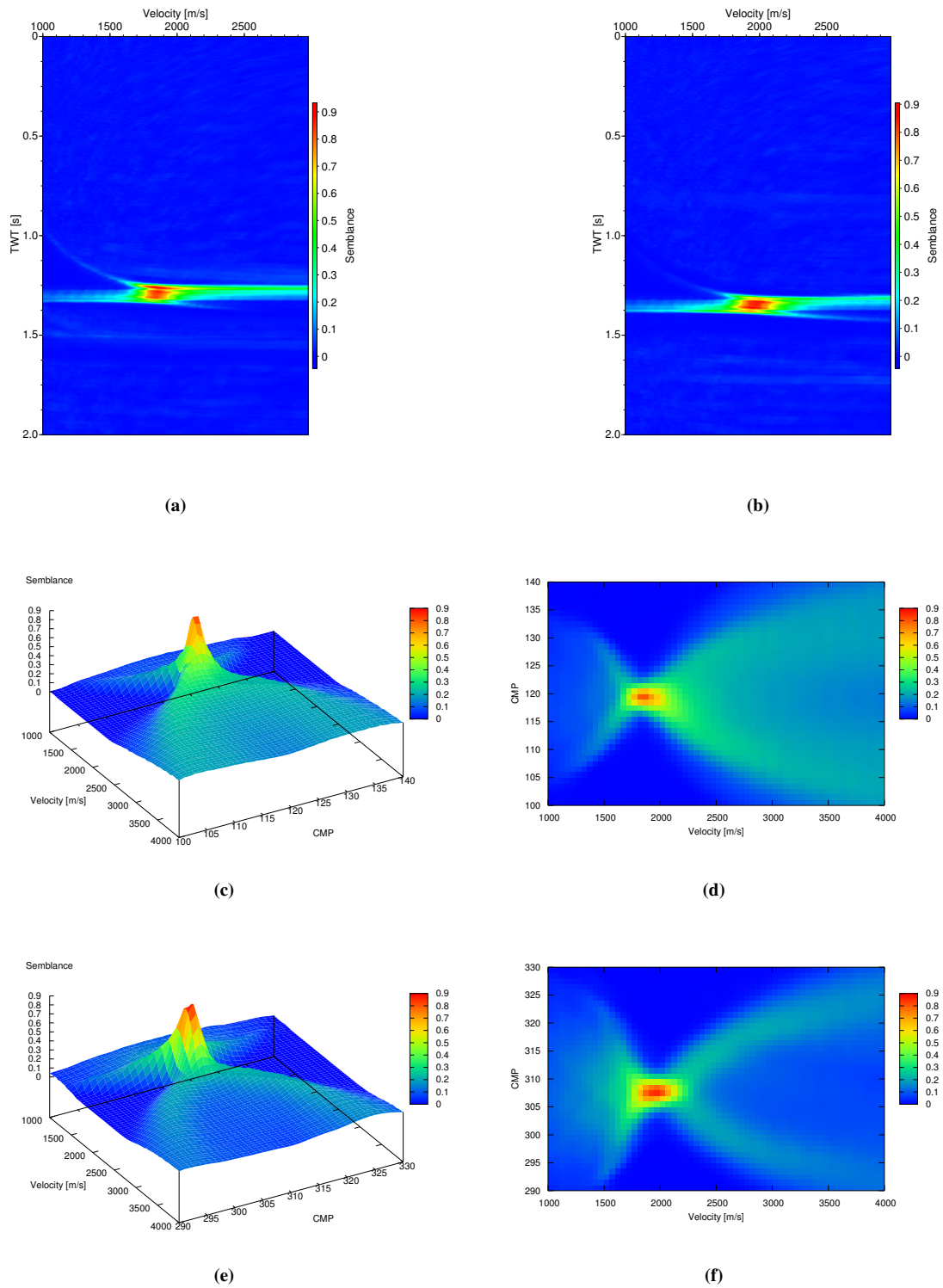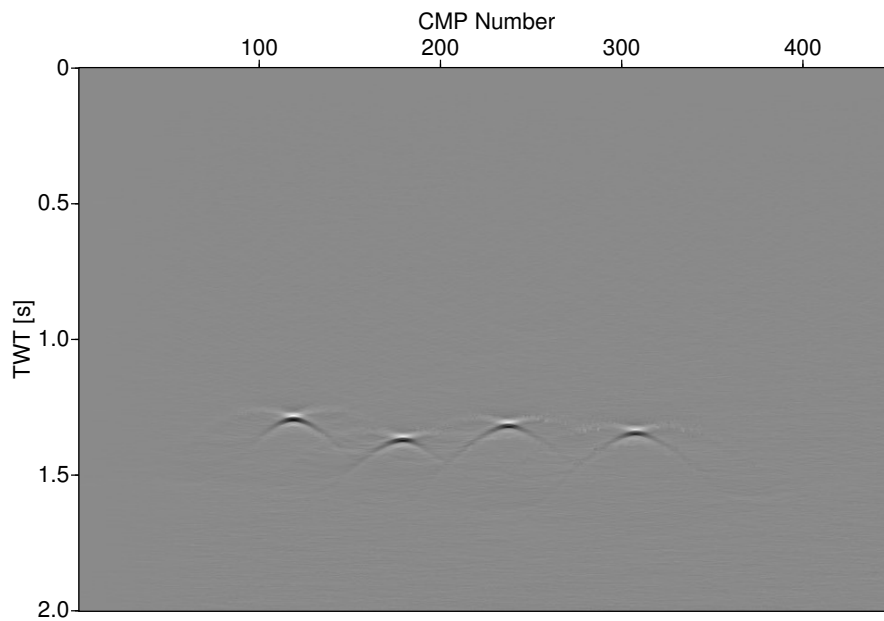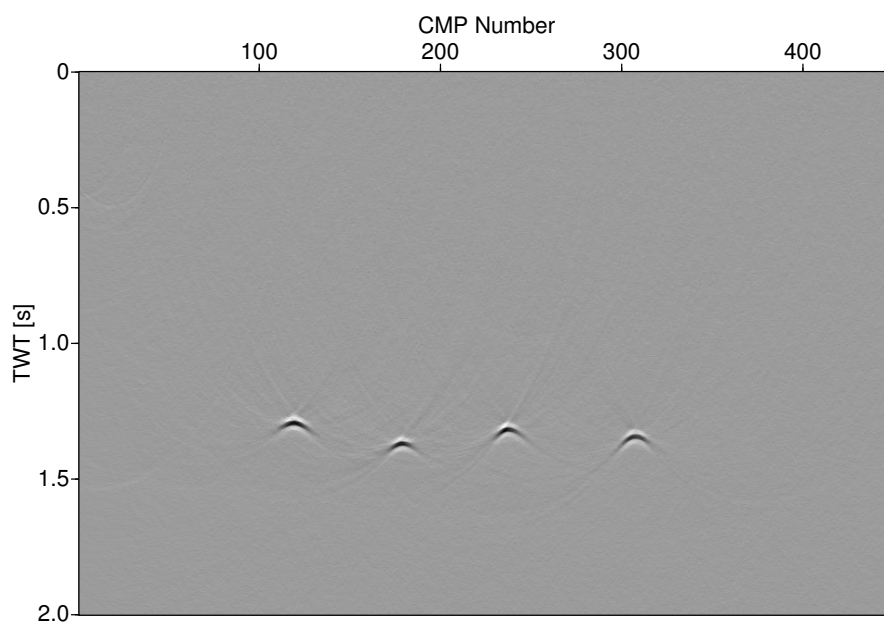
**Figure 2:** Velocity spectra for poststack migration velocity analysis by diffraction focusing of the synthetic model with 4 small lenses: CMP. 120 (a) and CMP 307. (b). CMPs are located directly over the scatter points. Red color indicates strong focusing, i.e. high semblance. The corresponding distribution of the coherence values for CMPs illustrated in (a) and (b). One observes sharp and narrow maxima for apexes of the diffractions.
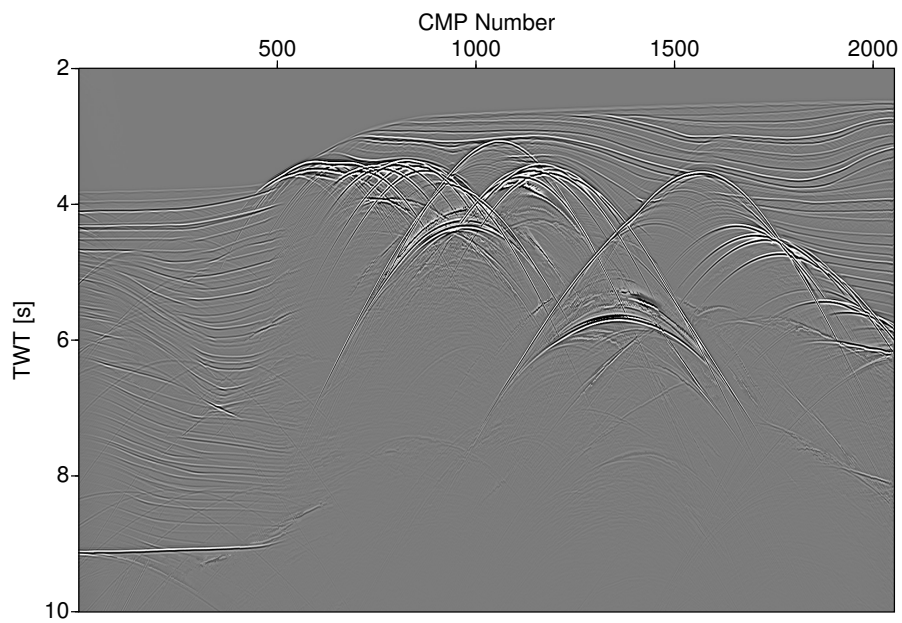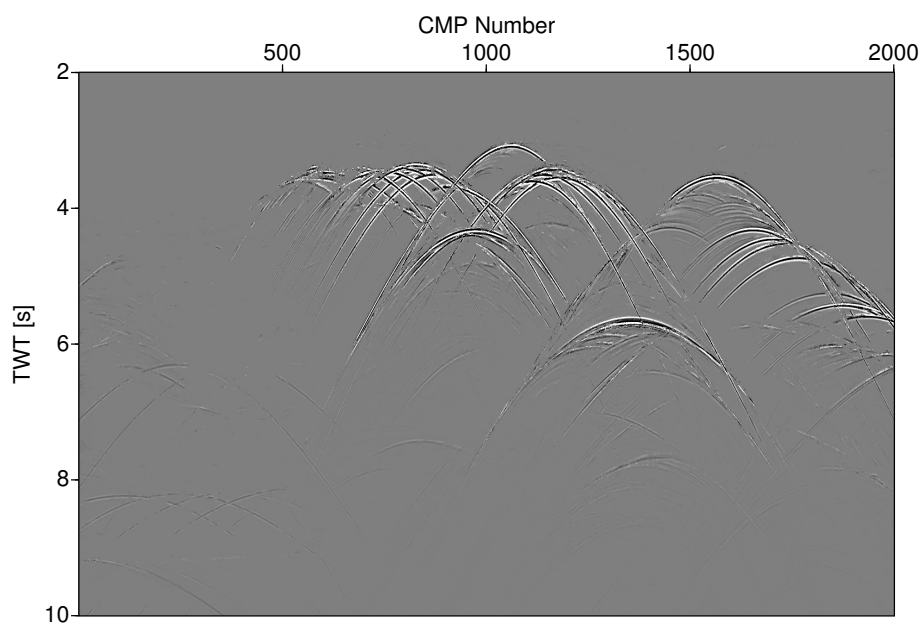
(a)



(b)

**Figure 3:** Poststack time migration of the diffraction only data of the synthetic model with five layers. Time migrated section obtained with the estimated RMS velocity (a) and the velocity model estimated on the diffraction only data (b).

**(a)**



**(b)**

**Figure 4:** Stacked section of the full wavefield (a) and diffraction only (b) for the synthetic Sigsbee2a model.
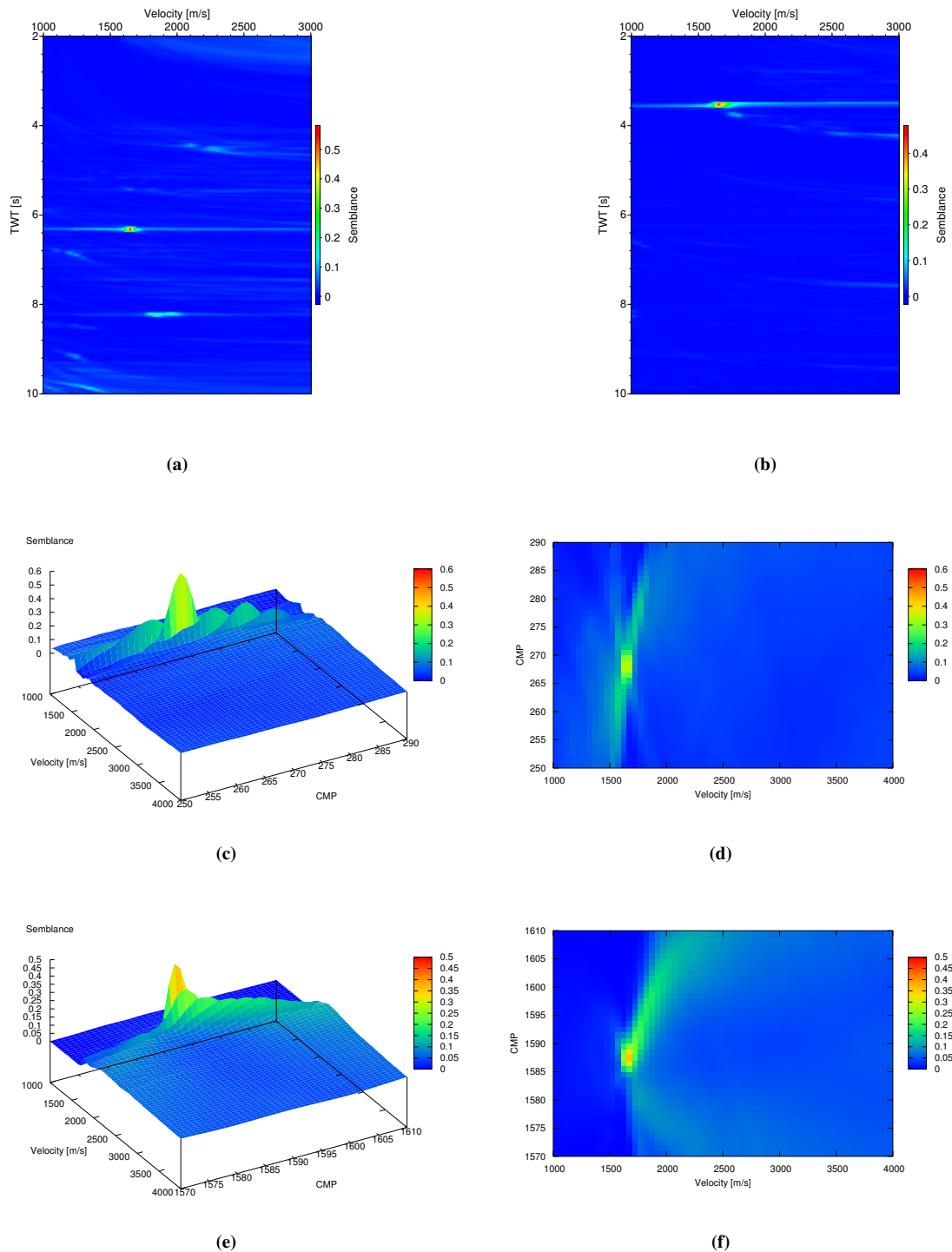
**Figure 5:** Velocity spectra for poststack migration velocity analysis by diffraction focusing of the synthetic model Sigsbee2a: CMP. 268 (a) and CMP. 1587 (b). CMPs are located directly over the scatter points. Red color indicates strong focusing, i.e. high semblance.The corresponding distribution of the coherence for CMPs illustrated in (a) and (b). We observe sharp and narrow maxima for apexes of the diffractions.
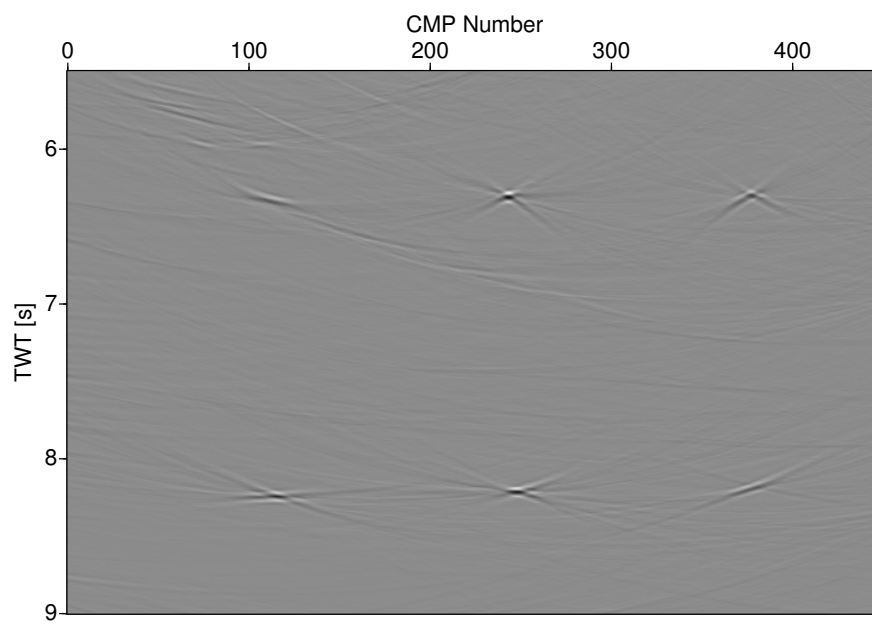
**(a)**
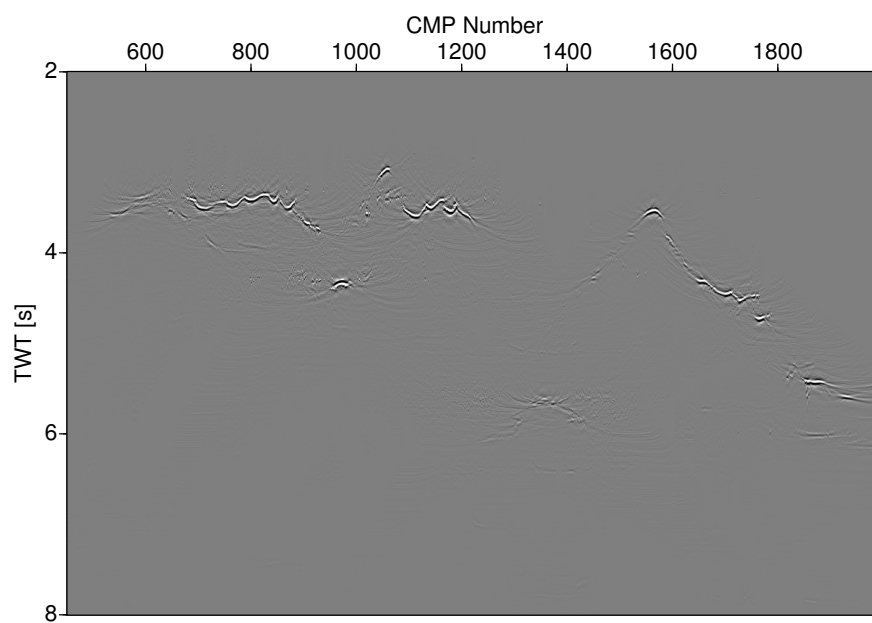


**(b)**

**Figure 6:** Poststack time migration of the diffraction only data for the synthetic Sigsbee2a model: (a) left part of the model, (b) right part of the model, where the scatterers build the sub salt.